AD

Technical Report ARAEW-TR-08007

TECHNOLOGY Exploitation/Exploration/Examination REPORT (TeX3) ADAPTIVE SELF-LUBRICATING NANOPOROUS HARD COATINGS

Christopher P. Mulligan

April 2008

ARMAMENT RESEARCH, DEVELOPMENT AND ENGINEERING CENTER
Armaments Engineering & Technology Center
Weapon Systems & Technology
Benét Laboratories

Approved for public release; distribution is unlimited.

The views, opinions, and/or findings contained in this report are those of the author(s) and should not be construed as an official Department of the Army position, policy, or decision, unless so designated by other documentation.

The citation in this report of the names of commercial firms or commercially available products or services does not constitute official endorsement by or approval of the U.S. Government.

Destroy this report when no longer needed by any method that will prevent disclosure of its contents or reconstruction of the document. Do not return to the originator.

REPORT DOCUMENTATION PAGE

Form Approved
OMB No. 0704-0188

PLEASE DO NOT RETURN YOUR FORM TO THE ABOVE ADDRESS.

1. REPORT DATE *(DD-MM-YYYY)*	2. REPORT TYPE	3. DATES COVERED *(From - To)*
xx-04-2008	Final	2008

4. TITLE AND SUBTITLE

TECHNOLOGY Exploitation/Exploration/Examination REPORT (TeX3)
ADAPTIVE SELF-LUBRICATING NANOPOROUS HARD COATINGS

5a. CONTRACT NUMBER

5b. GRANT NUMBER

5c. PROGRAM ELEMENT NUMBER

6. AUTHOR(S)

Mulligan, Christopher P.

5d. PROJECT NUMBER

5e. TASK NUMBER

5f. WORK UNIT NUMBER

7. PERFORMING ORGANIZATION NAME(S) AND ADDRESS(ES)

U.S. Army ARDEC, AETC
Benét Laboratories, AMSRD-AAR-AEW, B. 40
1 Buffington Street
Watervliet Arsenal, NY 12189-4000

8. PERFORMING ORGANIZATION REPORT NUMBER

ARAEW-TR-08007

9. SPONSORING/MONITORING AGENCY NAME(S) AND ADDRESS(ES)

U.S. Army ARDEC, AETC
Benét Laboratories, AMSRD-AAR-AEW, B. 40
1 Buffington Street
Watervliet Arsenal, NY 12189-4000

10. SPONSOR/MONITOR'S ACRONYM(S)

11. SPONSOR/MONITOR'S REPORT NUMBER(S)

12. DISTRIBUTION/AVAILABILITY STATEMENT

Approved for public release; distribution is unlimited.

13. SUPPLEMENTARY NOTES

14. ABSTRACT

The U.S. Army Technology Exploitation/Exploration/Examination (TEX3) Program is funding efforts to determine how recent advances in nanotechnology can be of benefit to the military. One particular area of interest is nanocomposite thin films and coatings, a source of considerable study in recent years. Nanocomposites generally combine one or more nanocrystalline phases in a functional matrix to provide improved mechanical properties, corrosion resistance, and/or thermal stability. One example of this is the combination of a soft solid lubricating phase with a hard wear resistant matrix to provide improved wear resistance. Solid lubrication is of significant interest due to the significant problems posed by use of conventional lubricants in desert environments. The goal of this work is to determine how deposition conditions relate to the morphological evolution of the nanostructure of a specific CrN-Ag model nanocomposite system and how these nanostructures correlate to mechanical and adaptive lubrication properties.

15. SUBJECT TERMS

Nanotechnology, Nanocomposites, Wear resistance, Lubrication

16. SECURITY CLASSIFICATION OF:			17. LIMITATION OF ABSTRACT	18. NUMBER OF PAGES	19a. NAME OF RESPONSIBLE PERSON
a. REPORT	b. ABSTRACT	c. THIS PAGE			19b. TELEPHONE NUMBER *(Include area code)*
U/U	U	U	U	23	

INSTRUCTIONS FOR COMPLETING SF 298

1. REPORT DATE. Full publication date, including day, month, if available. Must cite at least the year and be Year 2000 compliant, e.g. 30-06-1998; xx-06-1998; xx-xx-1998.

2. REPORT TYPE. State the type of report, such as final, technical, interim, memorandum, master's thesis, progress, quarterly, research, special, group study, etc.

3. DATES COVERED. Indicate the time during which the work was performed and the report was written, e.g., Jun 1997 - Jun 1998; 1-10 Jun 1996; May - Nov 1998; Nov 1998.

4. TITLE. Enter title and subtitle with volume number and part number, if applicable. On classified documents, enter the title classification in parentheses.

5a. CONTRACT NUMBER. Enter all contract numbers as they appear in the report, e.g. F33615-86-C-5169.

5b. GRANT NUMBER. Enter all grant numbers as they appear in the report, e.g. AFOSR-82-1234.

5c. PROGRAM ELEMENT NUMBER. Enter all program element numbers as they appear in the report, e.g. 61101A.

5d. PROJECT NUMBER. Enter all project numbers as they appear in the report, e.g. 1F665702D1257; ILIR.

5e. TASK NUMBER. Enter all task numbers as they appear in the report, e.g. 05; RF0330201; T4112.

5f. WORK UNIT NUMBER. Enter all work unit numbers as they appear in the report, e.g. 001; AFAPL30480105.

6. AUTHOR(S). Enter name(s) of person(s) responsible for writing the report, performing the research, or credited with the content of the report. The form of entry is the last name, first name, middle initial, and additional qualifiers separated by commas, e.g. Smith, Richard, J, Jr.

7. PERFORMING ORGANIZATION NAME(S) AND ADDRESS(ES). Self-explanatory.

8. PERFORMING ORGANIZATION REPORT NUMBER. Enter all unique alphanumeric report numbers assigned by the performing organization, e.g. BRL-1234; AFWL-TR-85-4017-Vol-21-PT-2.

9. SPONSORING/MONITORING AGENCY NAME(S) AND ADDRESS(ES). Enter the name and address of the organization(s) financially responsible for and monitoring the work.

10. SPONSOR/MONITOR'S ACRONYM(S). Enter, if available, e.g. BRL, ARDEC, NADC.

11. SPONSOR/MONITOR'S REPORT NUMBER(S). Enter report number as assigned by the sponsoring/ monitoring agency, if available, e.g. BRL-TR-829; -215.

12. DISTRIBUTION/AVAILABILITY STATEMENT. Use agency-mandated availability statements to indicate the public availability or distribution limitations of the report. If additional limitations/ restrictions or special markings are indicated, follow agency authorization procedures, e.g. RD/FRD, PROPIN, ITAR, etc. Include copyright information.

13. SUPPLEMENTARY NOTES. Enter information not included elsewhere such as: prepared in cooperation with; translation of; report supersedes; old edition number, etc.

14. ABSTRACT. A brief (approximately 200 words) factual summary of the most significant information.

15. SUBJECT TERMS. Key words or phrases identifying major concepts in the report.

16. SECURITY CLASSIFICATION. Enter security classification in accordance with security classification regulations, e.g. U, C, S, etc. If this form contains classified information, stamp classification level on the top and bottom of this page.

17. LIMITATION OF ABSTRACT. This block must be completed to assign a distribution limitation to the abstract. Enter UU (Unclassified Unlimited) or SAR (Same as Report). An entry in this block is necessary if the abstract is to be limited.

TECHNOLOGY Exploitation/Exploration/Examination REPORT (TeX3)

ADAPTIVE SELF-LUBRICATING NANOPOROUS HARD COATINGS

C.P. MULLIGAN

CONTENTS

ABSTRACT

The U.S. Army Technology Exploitation/Exploration/Examination (TEX3) Program is funding efforts to determine how recent advances in nanotechnology can be of benefit to the military. One particular area of interest is nanocomposite thin films and coatings. These materials have been a source of considerable study in recent years. Nanocomposites generally combine one or more nanocrystalline phases in a functional matrix to provide improved mechanical properties, corrosion resistance, and/or thermal stability. One example of this is the combination of a soft solid lubricating phase with a hard wear resistant matrix to provide improved wear resistance. Solid lubrication is of significant interest due to the significant problems posed by use of conventional lubricants in desert environments and by controlling the nanostructure of these materials it is possible to obtain adaptive solid lubricating properties, that is, the lubricant is directed to the layer surface during operation. Technology to produce nanocomposite coatings providing adaptive lubrication has been studied for a variety of applications and the goal of this work is to determine how deposition conditions relate to the morphological evolution of the nanostructure of a specific CrN-Ag model nanocomposite system and how these nanostructures correlate to mechanical and adaptive lubrication properties.

EXECUTIVE SUMMARY

For materials engineers, one of the most important goals is to obtain an understanding of how to manipulate microstructure and nanostructure to obtain desired material properties. As part of the U.S. Army's Technology Exploitation/Exploration/Examination (TEX3) Program, this study provides an investigation of nanostructured coatings to provide adaptive solid lubricating properties. Specifically, a nanocomposite coating consisting of a hard chromium nitride (CrN) matrix co-deposited with silver (Ag) is investigated. The premise of this coating system is that a solid lubricant layer of silver is present on the surface. As the solid lubricant layer is transferred to the wear surface and depleted, Ag diffuses out of the matrix to replenish the surface and maintain a low friction coefficient. The self-lubricating nature of this adaptive coating has the potential to extend the service lifetime of the coating in high and low temperature environments as well as in cyclic temperature use. Effective solid lubricating films are of considerable interest due to the problems posed by the use of conventional lubricants in desert environments, among other applications.

For this investigation, pure CrN baseline and CrN-Ag nanocomposite coatings were deposited via reactive magnetron sputtering under varying conditions. Characterization techniques were employed to determine the structure, mechanical, and tribological properties of these materials and correlations are made on how the deposition parameters can be used to manipulate the nanostructure and properties. Annealing studies were used to study the role of structure on the adaptive lubrication properties. These investigations determined that one of the most important factors in determining structure of these nanocomposite coatings is the substrate deposition temperature during film growth. The mobilities of atoms on the surface during deposition control the nanostructure of the film. Structural analyses indicate that the solid lubricant Ag segregates in the form of nanocrystalline platelets stretched parallel to the surface as growth temperature increase. This results in dramatic changes in to the overall nanostructure and thus properties.

Ability to control the nanostructure was demonstrated, and the properties of the nanocomposites were found to vary significantly with structure as expected. Initial room temperature tribological testing indicate significant improvements to friction and wear behavior for the appropriate structures and the annealing studies demonstrated the relationships between nanostructure, lubricant transport, and adaptive lubrication properties. Further work to build upon these initial studies is planned to fully exploit this technology for future applications.

I. Concept Background and Technology Applications

Corrosion and wear of military components is a significant problem facing today's armed services. As U.S. military operations in mid-east environments are increasing, new problems are emerging which necessitate the development of advanced wear and corrosion resistant materials. In particular, significant research is being conducted in the area of solid lubrication for weapon action and other military components as the use of conventional liquid lubricants poses significant problems in the desert environment. Other areas where solid lubrication is of particular interest include in the development of advanced oil-free turbo-machinery which can offer significant weight savings and boosts in efficiency of tank and helicopter engines, as well as for use in dry high-speed cutting and machining operations to eliminate the costs and health risks associated with cutting fluids.

To address the growing needs of the military in this area, advanced materials and coatings are required. The use of nanostructured and nanocomposite materials shows great promise in advancing the state-of-the-art in terms of wear and corrosion protection.

The overall objective of this specific research project is to study a new approach to adaptive solid lubrication by the use of self-lubricating nanocomposite hard coatings. Specifically, the goals are to develop the basic scientific understanding of (a) the critical parameters that govern thin film structure evolution on the nanoscale and (b) the adaptive solid lubricating properties of the chosen prototype nanocomposite system. This study combines soft, lubricating materials and hard, wear resistant materials in a single coating and uses the concept of adaptive-lubrication, that is, the lubricant is directed to the layer surface during operation. The important factors necessitating the combination of materials into a composite are related to the intrinsic advantages and disadvantages of the separate hard phase and soft phase. For example, hard transition metal nitride coatings such as titanium nitride and chromium nitride exhibit excellent wear resistance, high temperature strength, and stable thermochemistry but they are susceptible to high friction, frictional heating, and fracture under aggressive loadings. Conversely, lattice layered solid lubricants such as graphite and molybdenum disulfide and soft noble metals such as silver exhibit low friction due to their low shear strengths, but by themselves are susceptible to relatively high wear rates and gross plowing. The goal is to combine the low friction of the solid lubricant with the excellent mechanical properties of the hard matrix.

The key novelty of the concept is the use of nanopores to guide and transport a solid lubricant to the surface. The development of nanopores in transition metal nitrides during film growth has been studied by Gall et al.[1] The solid lubricant in this prototype system is silver (Ag), which is chemically inert and has a low shear strength even below 300 °C. Above its melting point, 962 °C, Ag acts as a liquid lubricant. For the ideal prototype system, the Ag is contained in a hard wear-resistant chromium nitride (CrN) coating that exhibits a nanoporous microstructure with a dense cap-layer. Since the Ag is chemically immiscible in the CrN matrix, it will form a composite structure. Initially, there will be a thin lubricant Ag layer on the top surface. As the Ag surface layer is depleted by wear, it will be replenished by Ag which is contained in the hard matrix coating which moves to the surface by rapid diffusion through the nanopores as illustrated schematically in cross-section in Figure 1. This soft-on-hard coating approach will avoid the high wear rate that would be observed in a pure Ag layer. In addition, the hard matrix coating resists plastic deformation and the consequent roughening effects that are common for monolithic soft coatings.[2,3] Also, illustrated in Figure 1b are the proposed mechanisms of diffusion of the lubricant during operation. The silver atoms diffuse first horizontally within a crystalline column, secondly they move vertically in the nanopores to reach the surface where the cap-layer is damaged due to wear. Finally, they diffuse on the surface to replenish the depleted lubricant layer. No diffusion occurs at areas of the coating where the lubricant surface layer is still present, since the undamaged cap-layer acts as a diffusion barrier. The different diffusion processes happen at two distinct length-scales: bulk diffusion occurs in the ~25 nm range, while diffusion through the nanopores and on the open surface is 1-20 μm, two orders of magnitude larger than bulk diffusion.

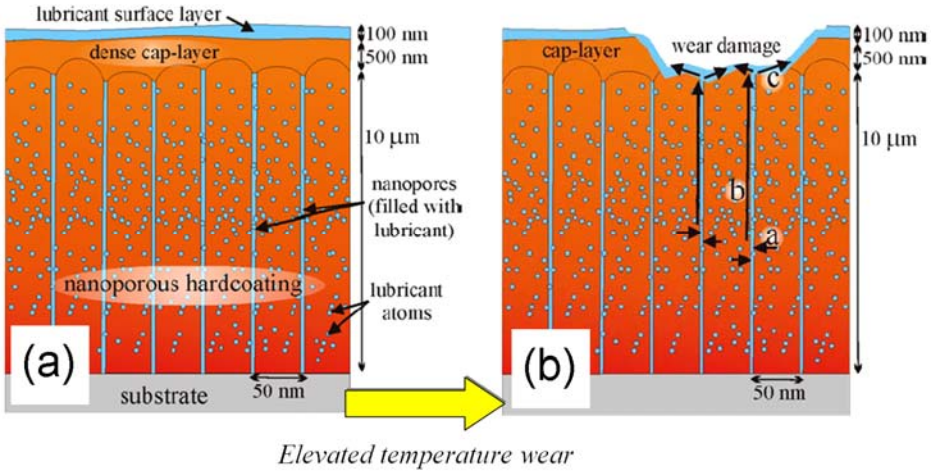

Figure 1: (a) Schematic of the concept for self-lubricating coatings. The wear-resistant hard coating contains soft lubricant atoms and exhibits nanopores which guide the lubricant to the surface during operation. (b) Schematic illustrating self-lubrication after wear damage, where lubricant atoms diffuse from the bulk with diffusion length length scale 'a' and through the nanopores with diffusion length scale 'b'.

The primary advantage of the proposed nanoporous coatings over isotropic or multilayered coatings will be the much smaller amount of wear that is required to initiate the supply of additional lubricant to the surface. For example, using the dimensions in Fig. 1, a wear scar which is 500 nm deep will cause a complete replenishing of the soft Ag-surface coating. In contrast, an isotropic coating where diffusion is limited, which contains a typical 10-20% of Ag and ~80-90% of a wear-resistant hard material,[2] would require a considerably deeper wear damage to set sufficient Ag free to replenish the depleted lubrication layer. Consequently, our new approach will result in a reduced amount of abrasive wear debris, which originates typically from the hard component in the coating. This, in turn, leads to an overall reduced wear rate and a dramatically extended coating lifetime.

While several recent studies have concentrated on similar combinations of materials and analysis of their properties based on the relative composition of phases,[4-9] relatively little has been done to understand and manipulate the nanostructure of these coatings to better obtain the desired adaptive properties. Obtaining this understanding is the goal of this research. In relating the deposition parameters to the nanostructures created, we will gain the ability to control the mechanical, tribological, and adaptive lubricating properties.

II. Results and Discussion

A. Experimental Procedure

CrN-Ag nanocomposite coatings were grown in a load-locked multi-chamber ultra-high vacuum (UHV) stainless-steel dc dual magnetron sputter deposition system with a base pressure of 1.3×10^{-7} Pa (1×10^{-9} Torr). Water-cooled 5-cm-diameter Cr and Ag targets with purities of 99.95% and 99.99%, respectively, were positioned at an angle of 45° with respect to the substrate surface normal as illustrated schematically in Figure 2. The substrates consist of metallographically polished 304 stainless steel and Si(001) wafers that were cleaned with successive rinses in ultrasonic baths of trichloroethane, acetone, and isopropanol and blown dry with dry N_2. The Si and steel substrates were mounted on a molybdenum sample

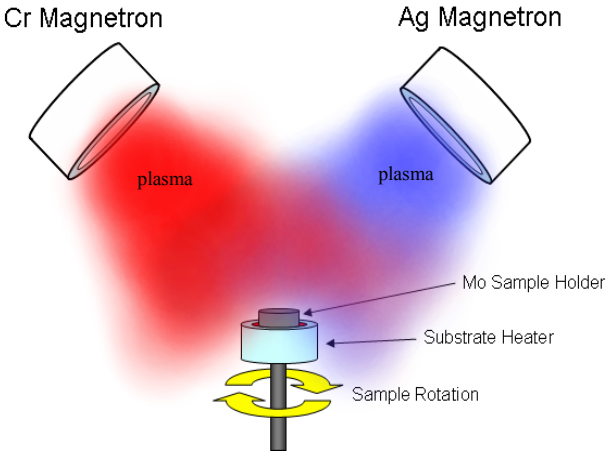

Figure 2: Schematic of substrate and magnetron orientation in deposition chamber.

holder using Pelco colloidal silver paste and inserted into the load-lock chamber for transport to the deposition chamber where they were heated with a resistive heater to the desired growth temperatures of T_s = 500, 600, or 700 °C. 99.999% pure N_2 was further purified using a Micro Torr purifier and introduced through metering valves to reach a constant chamber pressure of 0.4 Pa (3 mTorr), which was measured using a capacitance manometer. Just prior to initiating deposition, the targets were sputter cleaned for 5 minutes while the substrate was covered with a protective shutter. Sputtering was carried out at a constant power of 450 W to the Cr target, yielding a deposition rate of ~30 nm/min. The power to the Ag target was maintained at either 0 or 160 W, to grow pure CrN or coatings with 22 at.% Ag, respectively. The substrates were continuously rotated about the polar axis with 50 rpm, in order to obtain optimal coating uniformity. The deposition temperature, including the contribution due to plasma heating, was measured using a pyrometer which was cross-calibrated with a thermocouple within the sample stage.

X-ray diffraction (XRD) for structure determination was completed with a Scintag Diffractometer. Analysis of the composition and microstructure was completed using scanning electron microscopy (SEM) and energy dispersive spectroscopy (EDS). These analyses were performed in a JEOL JSM-840A SEM with a Kevex Instruments model 2003 detector as well as a JEOL JSM-6330F FE-SEM.

Hardness was measured with a Wilson-Tukon Microhardness Tester with a Knoop indenter operating at a 10g load. The system variation in hardness vs. load for the Knoop indenter was calibrated at loads of 10-200 g, using a 20-μm-thick TiN coating with similar hardness as the CrN-Ag nanocomposite coatings, in order to correlate the measured Knoop microhardness to the hardness in GPa. The hardness values were obtained by averaging over five indentations into metallographically polished cross-sections of 5-μm-thick nanocomposite layers.

To analyze the lubricant transport properties as a function of microstructure, vacuum annealing experiments were completed in the above described deposition system at 700 and 800 °C, for 5, 20, and 60 minutes, with a background pressure of less than 1×10^{-5} Pa.

Some initial room temperature tribological measurements were made, including friction coefficient and wear depths and rates of the coatings deposited on 304 stainless steel using a Nanovea Series pin-on-disk tribometer. The specimens were tested in air by sliding a 6 mm diameter 100Cr6 bearing steel ball with a hardness of 7.5 GPa at a rate of 10 cm/s, a normal load of 15 N, for 10,000 cycles. Friction coefficients were recorded continuously throughout testing. The wear scars were analyzed using a Nanovea ST400 non-contact optical profilometer.

B. Coating Composition and Structure

The relative deposition rates of pure CrN and pure Ag, grown in a N_2 atmosphere as a function of dc power, were determined by thickness measurements using SEM cross-sectional microscopy. Based on these results, the power input to the Ag target was adjusted to obtain the desired composition with an Ag content of 22 at.%. Post-deposition EDS analyses verified the desired composition, which was chosen as a basis for comparison to previous studies.[10,11] Based on CrN and Ag molar volumes of 11.2 and 10.3 cm^3/mol, respectively, this corresponds to a volume fraction of solid lubricant in the matrix phase of 34.1 vol.%. The CrN within the composite is expected to be stoichiometric based on the chosen deposition conditions which correspond to those of previous investigations.[1,12]

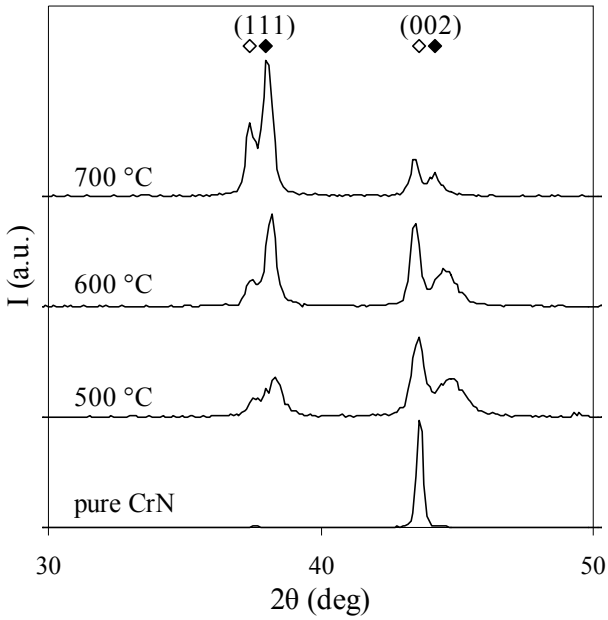

Figure 3: XRD θ-2θ scans from pure CrN and CrN-Ag composite coatings deposited at 500, 600, and 700 °C. The expected positions for CrN and Ag 111 and 002 reflections are indicated.

Fig. 3 shows X-ray diffraction scans from pure CrN grown at 600 ºC and from CrN-Ag composite coatings deposited at 500, 600, and 700 °C. The most prevalent peaks within the scan range of 5 to 140 °2θ are from 111 and 002-typ reflections. The 111 and 002 peaks for pure CrN, appear at 37.60 and 43.65 °2θ, respectively. The 002 peak has a full-width at half-maximum (FWHM) of 0.35° and an intensity that is 100× stronger than the 111 peak, indicating a highly preferred 002 orientation. In contrast, the CrN-Ag composite coatings have 002 and 111 reflections with comparable intensity and also exhibit 220 and 311peaks (not shown), indicating a mixed grain orientation. With increasing growth temperature, the 111-vs-002 intensity ratio increases from 0.24× to 0.31× to 2.0× while the FWHM of the CrN(002) peak decreases from 0.59° to 0.43° to 0.41°, for T_s = 500, 600 and 700 °C, respectively. The FWHM for the Ag(111) and Ag(002) peaks show a comparable trend, decreasing from 0.78 and 1.12 °2θ at T_s = 500 ºC to 0.44 and 0.82° at T_s = 600 ºC and 0.45 and 0.43° at T_s = 700 ºC, respectively. The Ag(002) peak shifts from 44.79° to 44.59° to 44.28°, for T_s = 500, 600, and 700 ºC, respectively. The values are smaller than the expected bulk position of 44.28º for T_s = 500 and 600 ºC, while that

for T_s = 700 ºC values matches up well. The larger peak shifts associated with lower T_s indicate a reduced interplanar spacing aligned with the substrate normal. This strain can likely be attributed to a tensile strain parallel to the surface from the considerable thermal expansion coefficient mismatch between CrN (~7×10^{-7} /ºC) and Ag (~1.9×10^{-5} /ºC). As the coating cools from the growth temperature to ambient temperature, the Ag is trapped between CrN grains and restrained from fully contracting. However, at higher growth temperatures the XRD data suggests that the Ag grain size is increasing and tensile strain is decreasing. Larger Ag grains indicate increased segregation and these larger Ag grains are no longer constrained by the CrN matrix and are allowed to fully relax as is the case for T_s = 700 ºC.

The XRD results show that the addition of Ag to the growth of CrN leads to a transition from a nearly perfect 002-texture to a mixed layer orientation. This is attributed to Ag at the growing layer surface causing re-nucleation of CrN grains with random orientation. As growth temperature increases, the 111-oriented grains of both CrN and Ag become increasingly dominant. This is associated with an increased adatom mobility that results in Ag precipitates (as discussed below) which, at elevated temperatures, preferentially align to expose low-energy Ag(111) surfaces that, in turn, are the nucleation sites for 111-oriented CrN sites. The decreasing XRD peak width with increasing T_s is attributed to the increasing Ag segregate size that reduces the number of CrN nucleation sites for a constant Ag content, which increases the CrN grain size.

Figure 4 shows cross-sectional backscatter electron micrographs from polished CrN-Ag coatings. The backscatter electron (BE) imaging mode yields elemental contrast with the higher-atomic-mass Ag appearing bright in the dark CrN matrix. The BE image for the layer grown at T_s = 500 ºC (Fig. 4(a)) shows a uniform contrast, indicating that the size of the Ag precipitates are below the detection resolution in the backscatter mode ($\leq$ 25nm). The secondary electron image from the same sample shown on the right in Fig. 4(a) confirms the relatively homogeneous microstructure. In contrast, the micrograph in Fig. 4(b) from the layer grown at 600 ºC exhibits well developed Ag grains that extend parallel to the layer surface to form lamella with an average size of ~$300\times300\times100$ nm^3. Fig. 4(c) shows that a further increase in the growth temperature to T_s = 700 °C causes Ag lamellar grains to further segregate into alternating Ag rich and Ag depleted zones within the CrN matrix, with the average lamella size increasing to ~$600\times600\times200$ nm^3. We attribute the increase in Ag grain size with T_s to a temperature-activated surface mobility that allows Ag to nucleate submicron precipitates on the growing layer surface. The extension perpendicular to the growth direction is likely associated with Ag precipitates

forming as platelets on the layer surface that are subsequently overgrown by renucleated CrN grains.

An additional effect of increasing growth temperature is the formation of large nodular defects in the film as depicted in Figure 5. SEM cross-section micrographs for T_s = 500, 600, and 700 °C are given in Fig. 5(a), (b), and (c), respectively. The images illustrate the increase in large outgrowths as a function of growth temperature. These periodic structures occur from the segregation of large (up to 2000×2000×4000 nm^3) Ag precipitates out to and along the surface during deposition due to the very high Ag adatom mobilities. BE images showing the contrast between the large Ag precipitates and the CrN matrix are given in Figure 6. Fig. 6(a) and (b) illustrate the large Ag precipitate at the base of the defects for T_s = 600 and 700 °C, respectively. No such defects occur at 500 °C.

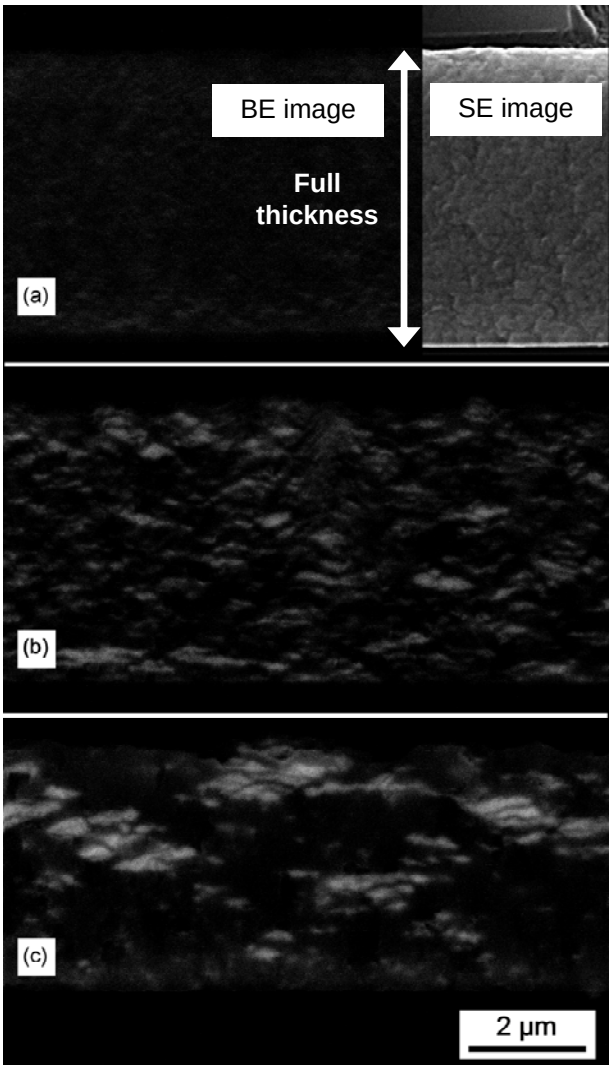

Figure 4: Cross-sectional BE-SEM micrographs from 22 at.% Ag specimen deposited at (a) 500 °C (b) 600 °C, and (c) 700 °C. Inset in (a) is the corresponding SE image showing the fine grained structure.

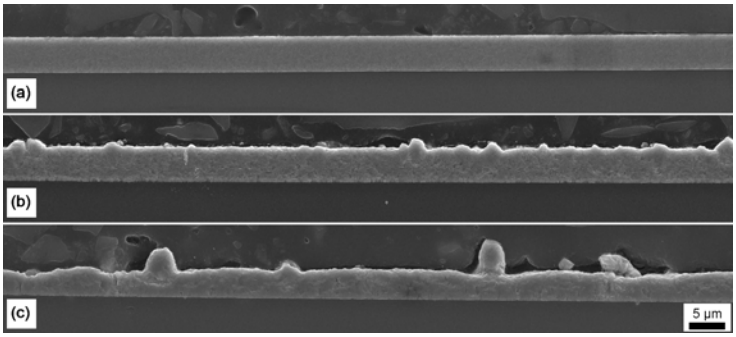

Figure 5: SEM cross-sectional micrographs for coatings deposited at (a) 500 °C (b) 600 °C, and (c) 700 °C. Note the increase in large outgrowths with increasing T_s.

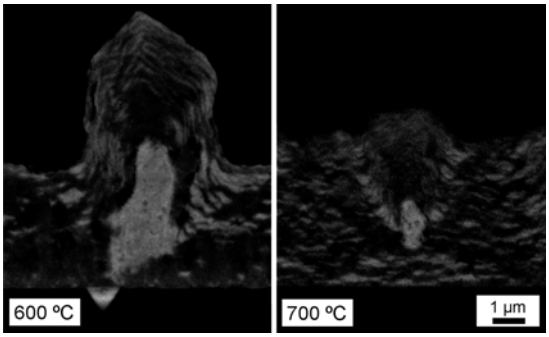

Figure 6: BE cross-sectional micrographs for coatings deposited at (a) 600 °C and (b) 700 °C showing large Ag precipitates at base of defects.

C. Lubricant transport to the surface

CrN-Ag composite coatings were annealed in order to study the diffusive transport of the Ag solid lubricant to the surface. Figure 7 is a typical plan-view SEM micrograph from a 22%-Ag coating which was annealed at 700 °C for 60 minutes. The Ag that diffused to the surface appears as bright particles in the micrograph. The compositional map, obtained by EDS X-ray dot-mapping from the outlined area, is shown in Fig. 7(b). It confirms that these particles are Ag aggregates. The dark spots correspond to areas with high Ag concentration while the bright background indicates Cr. The Ag particles are uniformly distributed on the surface.

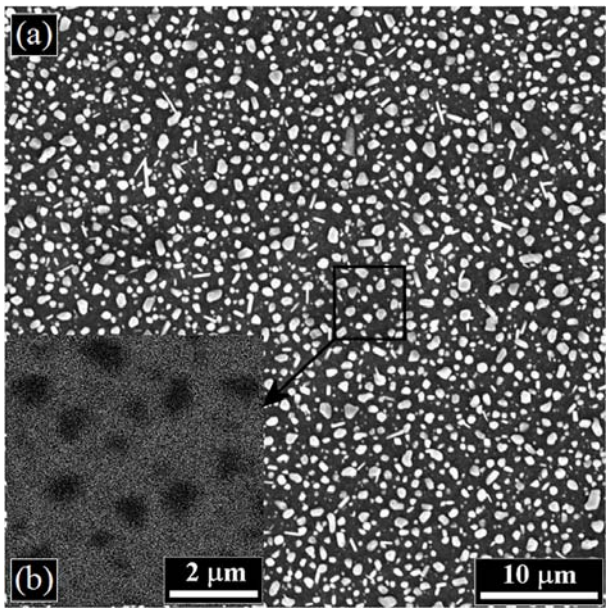

Figure 7: (a) Secondary electron micrograph and (b) corresponding higher magnification EDS X-ray dot map from a surface of a CrN-Ag composite coating with 22 at.% Ag that was annealed for 60 minutes at 700°C. The composition map is obtained from the outlined area and shows Ag as dark and Cr as bright dots.

The lubricant transport was analyzed as a function of structure by annealing the nanocomposite coatings deposited with T_s = 500, 600, and 700 °C. Figure 8 gives plan-view micrographs of the various coatings annealed for 20 minutes at 700 °C. The as-deposited surface morphologies for T_s = 500, 600, and 700 °C are given in Fig. 8(a), (b), and (c), respectively, while the surface morphologies post annealing are given directly below those in Fig. 8(d), (e), and (f). The mounds present in the micrographs for T_s = 600 and 700 °C are the same as those captured in cross-section in Fig. 5 and 6 where large Ag precipitates have segregated at the surface during deposition. Following annealing it is clear that for the fine grained nanostructure of the coating deposited at 500 °C, the rate of lubricant transport is much higher than for that of the larger grained structures deposited at 600 °C and 700 °C. In fact, there is ~50% less Ag at the surface for the 600 °C sample vs. 500 °C and the 700 °C shows no appreciable Ag transport at all. To determine if the lubricant transport for T_s = 700 °C could be thermally activated at a $T > T_s$, the sample was also annealed at 800 °C for 60 minutes. At the elevated annealing temperature and for an extended period of time, still no transport of Ag to the surface was observed. This

clearly shows the strong correlation between nanocomposite structure and lubricant transport. The significant changes in lubricant transport properties can likely be attributed to two factors. First, the increased segregation of the Ag at elevated temperature leads to a structure where the diffusion pathway to the surface is obstructed by alternating regions of relatively dense CrN deficient in Ag and those regions rich in Ag. While for that of the homogeneous fine grained nanostructure, the diffusion path should be relatively continuous, with the Ag contained primarily in the columnar nanopores between CrN grains. Secondly, the thermodynamic driving force for transport and coarsening of Ag grains at the surface would decrease as the Ag grain size within the matrix increases. For the smaller grains, the overall amount of surface area of Ag within the matrix is higher leading to higher surface energy. Coarsening of Ag particles within the CrN matrix is restrained by the size of the nanopores so Ag must flow out of the hard matrix to increase grain size and decrease surface energy and as the Ag near the surface escapes, the result is a concentration gradient, which would result in further Ag diffusion.

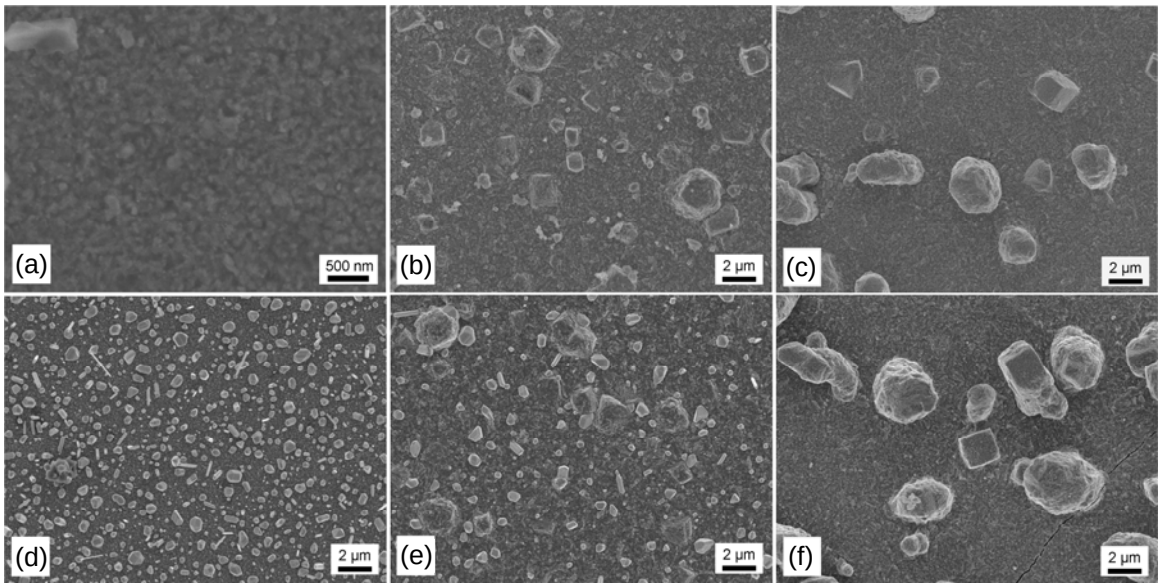

Figure 8 SEM plan-view micrographs for coatings in the as-deposited condition at (a) 500 °C (b) 600 °C, and (c) 700 °C and the same coatings after a 20 min. anneal at 700 °C in (d), (e), and (f). Note the formation of Ag grains at the surface for T_s = 500 and 600 °C, while no Ag has diffused to the surface for T_s = 700 °C.

The SEM investigations presented in Fig. 7 and 8 show that the lubricant transport of Ag to the surface can be controlled by manipulation of the nanocomposite structure. The process of lubricant transport is exactly what is envisioned for the CrN-Ag self-lubricating coating system and the ability to control it is paramount to designing adaptive coatings for the appropriate environment. The ability to control the nanostructure and related lubricant transport coupled with

the varying properties as a function of solid lubricant concentration illustrated in previous studies[10,11] provide a framework for custom design of adaptive nanocomposite coating systems.

At this point, it is also worthy to note that the control of the nanostructure for this nanocomposite system extends beyond just the current model of adaptive lubrication. By substituting different functional materials as the matrix and inclusion phases, specialized nanocomposite coatings to address issues ranging from chemical corrosion to thermal management (e.g. thermal barrier coatings) can be envisioned.

D. Mechanical and Tribological Properties

Figure 9 is a plot of the measured cross-sectional microhardness, H, as a function of deposition temperature for a pure CrN sample and for the three CrN-Ag layers with 22 at.% Ag. Pure CrN exhibits a microhardness of 28.2 GPa, within the range of previously reported values ranging from 17 to 30.[13-15] The composite coatings have lower H values, which increase with T_s from 16.5 to 19.7 to 24.3 GPa for T_s = 500, 600, and 700 °C, respectively, in good agreement with previous results on similar layers.[10] The increase in average H with T_s is attributed to Ag segregation of large grains to the surface during deposition as was illustrated in Fig. 6, leading to a lower effective concentration of Ag within the rest of the CrN matrix. The Ag segregation also leads to increased variations of the measured H values. This is due to the increased inhomogeneity of the structure with T_s and the formation of alternating Ag rich and Ag depleted zones, as discussed previously. The Ag-depleted zones are considerably harder than Ag rich zones. The error bars in the graph in Fig. 9 represent the standard deviation of the measured hardness values for multiple indentations into the same sample. The error bars increase with T_s, that is, they increase with increasing inhomogeneity. The error bar for the T_s = 500 ºC layer is comparable with that for the pure CrN, indicating the homogeneity of its microstructure.

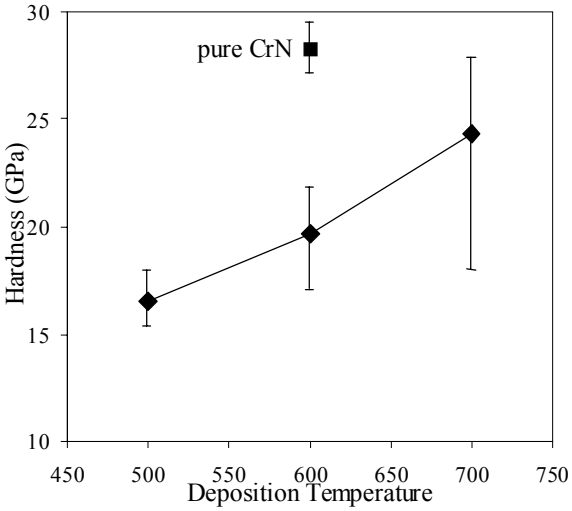

Figure 9: Plot of hardness vs. deposition temperature for pure CrN and CrN-Ag nanocomposite coatings.

Fig. 10 is a plot of the friction coefficient μ, determined by pin-on-disk measurements, for CrN-Ag nanocomposite coatings deposited on stainless steel substrates at substrate

temperatures of 500, 600, and 700 °C. The plot also includes the friction data for a pure CrN sample. All coatings tested were ~5μm thick and subjected to 10000 cycles for a total sliding distance of 377 m. The initial average surface roughness (R_a) for the pure CrN iss 12 nm, while the composites give R_a = 28, 174, and 961 nm for T_s = 500, 600, and 700 °C. The pure CrN specimen displayed an initial friction coefficient of ~0.7 followed by a drop to an average of 0.64 after a 1000 cycle running-in period, in close agreement with reported values for CrN with steel counterface.[15] All CrN-Ag composite samples displayed an initial friction coefficient of ~0.5 followed by fast rise in friction coefficient during the running-in period. The 500 and 600 °C deposited coatings dropped to average steady state friction coefficients over the final 5000 cycles of 0.58 and 0.47 respectively, while the 700 °C deposited coating exhibited a relatively high average friction coefficient of 0.85.

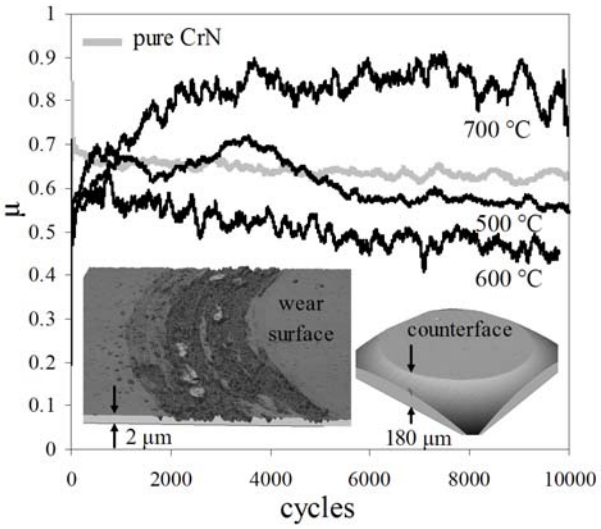

Figure 10: Plot of friction coefficients as a function of the number of cycles during pin-on-disk testing for pure and composite films. Inset – typical wear surface for both coating and counterface.

The wear rates of all coatings were calculated from 3-D profilometer surface topography data as illustrated in Fig. 10-inset. Average values were obtained by analysis of two segments of wear track located 180° from each other of 2.5 mm in length for each sample. Total wear volumes were taken within the each segment and extrapolated around the entire diameter to give the wear rate. The wear volumes and wear track widths are uniform around the circumference to within ±5% for each sample.

The average wear track width is 1.24 mm for pure CrN, while those for the nanocomposites are 1.11, 1.21, and 1.25 mm for T_s = 500, 600, and 700 °C respectively. The wear tracks conform to circular wear scars on the steel ball counterface (see Fig. 10-inset) of identical diameter to the measured track width. The reduced track widths for T_s = 500 and 600 °C are likely due to lower hardness of the nanocomposite resulting in less wear of the steel ball. The pure CrN coating exhibited an average wear rate of 3.6×10^{-6} mm^3/Nm, while the nanocomposites exhibited wear rates of 3.8×10^{-6}, 2.3×10^{-7}, and 9.9×10^{-6} mm^3/Nm for T_s = 500, 600, and 700 °C respectively. The variations in friction coefficient and wear rate are believed to be due to the orientation and structure of the Ag within the nanocomposite. For the 600 °C

nanocomposite deposition compared to pure CrN, the average friction coefficient is ~25% lower and the wear rate decreases by greater than an order of magnitude even with an average initial surface roughness 15× higher for the composite. This suggests the presence of distributed Ag inclusions of suitable size and orientation relative to the surface provide an effective solid lubricating interface. Conversely, for the 500 °C nanocomposite, there is relatively little difference in friction coefficient and wear rate. In this case the very fine grained Ag within the matrix does not form an effective and continuous interface and thus the coating behaves more like pure CrN. For the case of the 700 °C, there is actually a significant rise in friction coefficient and wear rate vs. pure CrN, likely due to the increased roughness and inhomogeneity in structure. The Ag grains are, in effect, too large for this nanocomposite and with the presence of the nodular defects as discussed previously, the material is worn too easily, leaving behind a roughened surface and generating a significant amount of wear debris.

This promising data summarized in Table I represents only an initial look into the tribological properties of the coatings. For an analysis of the adaptive properties of the films where the Ag solid lubricant is expected to have an even greater impact on friction and wear properties, tribological testing as a function of temperature is required. At elevated temperature, the advantages of the adaptive nanostructure will be fully utilized. This work is to be completed in follow-on efforts.

Table I. Mechanical and tribological properties of films

Sample	Pure CrN	500 ºC	600 ºC	700 ºC
Ag grain size (nm)	-	< 25	300×300×100	600×600×200
Hardness (GPa)	28.2	16.5	19.7	24.3
Friction Coeff. (μ)	0.64	0.58	0.47	0.85
Wear rate (mm^3/Nm)	3.6×10^{-6}	3.8×10^{-6}	2.3×10^{-6}	9.9×10^{-6}

III. ROI/Cost Analysis of Further Efforts

Wear and corrosion of materials is so prevalent and universal it is difficult to give a quantitative analysis of the tremendous costs they entail. A 2002 study by the U.S. Department of Transportation estimated that the direct cost of metallic wear and corrosion related problems alone is approximately $275 billion per year for the U.S.[16] Of course, these problems with wear and corrosion extend to the military. While these costs cannot be entirely eliminated, technologies that provide even marginal improvement in the lifecycle costs associated with wear and corrosion bring the potential for enormous cost savings.

In addition to the acquisition costs associated with the wear of military components, the performance aspect must be taken into account as well. Advanced nanocomposites will play a

role as enabling technologies for programs such as the Lightweight Small Arms Technology Program, where specialized materials are needed to provide thermal management within the chamber for caseless ammo technology and to provide for better performance in dusty conditions.[17] In terms of reliability, a 2007 West Point study showed statistics that indicate the rate of failure of the M4 is roughly 5× faster in sand/dust environments vs. normal ambient conditions,[18] and one of the major factors leading to failure of M16 and M4 weapons is the role of conventional lubricants attracting and accumulating dust in weapon action components.[19] Efforts to increase the performance and reliability of military components and to lessen the logistical burden on the soldiers are paramount to ensuring the continued safety and effectiveness of military personnel. Introducing advanced materials such as adaptive nanocomposites can play a significant role in these efforts.

For the case of the advanced nanocomposite coatings analyzed for this study, the costs associated with further efforts entail two phases. The first phase involves complete testing of the tribological properties of the materials within relevant temperature and atmospheric regimes and subsequent optimization of the coating system itself. Following optimization, development of coating deposition chambers capable of producing coatings on complex parts can be produced. Optimization parameters of particular interest include: total coating thickness, dense cap-layer thickness, Ag-content (atomic %), and nanopore width and density. Also envisioned are more complex structures which may include gradual composition changes or multilayers consisting of alternating nanoporous reservoirs and diffusion barrier layers to further prolong life. Additonal materials will also be explored for the replacement of the prototype materials, CrN and Ag, and effects on adaptive properties and performance will be analyzed. Other additions such as CaF_2 as an additional high-temperature lubricant to the CrN-Ag coatings by simultaneous deposition from Cr, Ag, and CaF_2 targets will be explored. Other alternative materials will be nitrides that form lubricious oxides at high temperature such as VN. The replacement of CrN by $Ti_{0.5}Al_{0.5}N$ and $Cr_{0.5}Al_{0.5}N$ and multilayers of these materials will also be studied which will likely lead to further enhancements in wear-resistance.

A cost estimate of phase I is given below. The estimate includes a total of 1.5-2 man years of labor and associated material and equipment costs. One senior engineer will work 100% on the project, for a total time of 1 year. The engineer will complete all depositions of coatings in available deposition chambers at Benet Labs and Rensselaer Polytechnic Institute (RPI). The engineer will utilize a variety of Benet's and RPI's central materials characterization facilities for microstructural and microchemical analysis. The engineer will work in close collaboration with

thin films and coatings expert, Prof. Daniel Gall, on deposition of layers as well as with tribology expert, Prof. Thierry Blanchet, on tribological investigations. The following list shows the expected schedule. Some overlap of the various scheduled tasks is desired to maximize the efficiency of the execution.

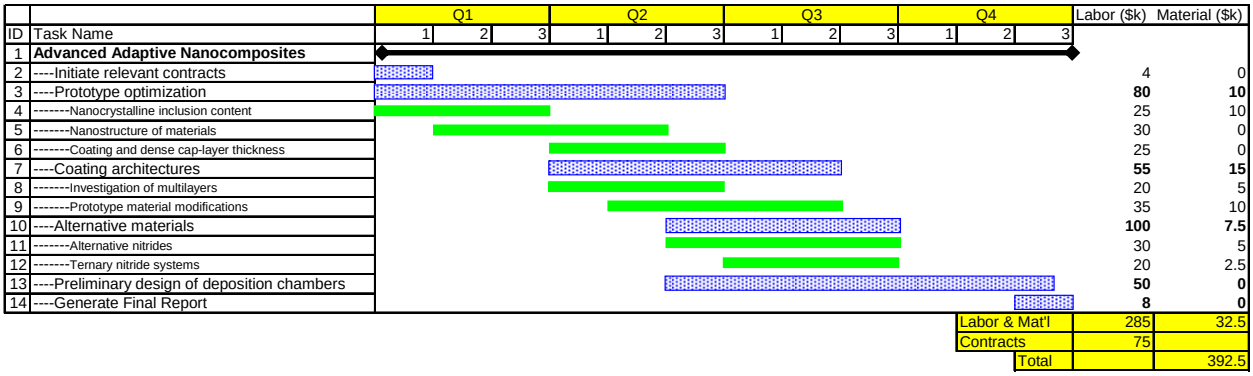

ID	Task Name	Labor ($k)	Material ($k)
1	**Advanced Adaptive Nanocomposites**		
2	----Initiate relevant contracts	4	0
3	----Prototype optimization	**80**	**10**
4	-------Nanocrystalline inclusion content	25	10
5	-------Nanostructure of materials	30	0
6	-------Coating and dense cap-layer thickness	25	0
7	----Coating architectures	**55**	**15**
8	-------Investigation of multilayers	20	5
9	-------Prototype material modifications	35	10
10	----Alternative materials	**100**	**7.5**
11	-------Alternative nitrides	30	5
12	-------Ternary nitride systems	20	2.5
13	----Preliminary design of deposition chambers	**50**	**0**
14	----Generate Final Report	**8**	**0**
	Labor & Mat'l	285	32.5
	Contracts	75	
	Total		392.5

IV. Cost/Benefit Potential of Leveraging of Other Agencies/industry Efforts

There exists several opportunities for collaboration and leveraging of other efforts. During this effort, close ties to Rensselaer Polytechnic Institute were developed and future work would be planned in collaboration with Prof's Daniel Gall and Thierry Blanchet. Significant work in the area of adaptive nanocomposites for the aerospace industry is being completed by personnel of the Air Force Research Laboratory (AFRL) and Southern Illinois University. Contact with personnel at AFRL and SIU has already been initiated. Additionally, Benet Laboratories has a close working relationship with the Institute of Tribology and Coatings (ITC) including a CRADA. ITC currently is conducting work under a contract to survey and identify the wear problems being experienced in the field. The outcome of this survey will help identify the components exhibiting the highest failure rates and most severe consequences and thus in most need of advanced coatings. This work will feed into the development and testing of materials as well as assist in identifying and designing appropriate deposition chambers in Phase II. Additionally, the principle investigators would work with development programs such as the Lightweight Small Arms Technology (LSAT) Program, and departments such as the National Small Arms Center (NSAC).

V. Acknowledgments

The author would like to thank Professors Daniel Gall and Thierry Blanchet of RPI for continuous guidance and assistance with structural analyses and tribological characterization and Dr. Sabrina Lee of U.S. Army Benet Laboratories for assistance with X-Ray diffraction. The author also thanks the U.S. Army TEX3 Program for supporting this effort.

VI. References

1. D. Gall, C.-S. Shin, T. Spila, M. Odén, M.J.H. Senna, J.E. Greene, and I. Petrov, *J. Appl. Phys*. 91 (2002) 3589.
2. B. Bhushan and B.K. Gupta, Handbook of tribology (Krieger Publishing, Malabar FL, 1997).
3. H.E. Sliney, ASLE Trans. **29**, 370 (1986).
4. P. Basnyat, B. Luster, Z. Kertzman, S. Stadler, P. Kohli, S. Aouadi, J. Xu, S.R. Mishra, O.L. Eryilmaz, A. Erdemir, Surface and Coatings Technology, 202 (2007) 1011.
5. Voevodin, J. J. Hu, J. G. Jones, T. A. Fitz, J. S. Zabinski, Thin Solid Films, 401 (2001) 187.
6. Muratore, J. J. Hu, A. A. Voevodin, Thin Solid Films, 515 (2007) 3638.
7. Muratore, A. A. Voevodin, J. J. Hu, J. S. Zabinski, Wear, 261 (2006) 797.
8. S. M. Aouadi, A. Bohnhoff, M. Sodergren, D. Mihut, S. L. Rohde, J. Xu, S. R. Mishra, Surface and Coatings Technology, 201 (2006) 418.
9. A.A. Voevodin, J.J. Hu, T.A. Fitz, J.S. Zabinski, Surface and Coatings Technology, 146–147 (2001) 351.
10. K. Kutschej, C. Mitterer, C.P. Mulligan, and D. Gall, Advanced Engineering Materials, 8 (2006) 1125.
11. C.P. Mulligan and D. Gall, Surf. Surface and Coatings Technology, 200, (2005) 1495.
12. Z.B. Zhao, Z.U. Rekb, S.M. Yalisovec, J.C. Bilelloc, Surface & Coatings Technology 185 (2004) 329.
13. S. Carrera, O. Salas, J.J. Moore, A. Woolverton, E. Sutter, Surface and Coatings Technology, 167 (2003) 25.
14. T. Polcar, N.M.G. Parreira, R. Novak, Surface and Coatings Technology, 201 (2007) 5228.
15. H.C. Barshilia, N. Selvakumar, B. Deepthi, K.S. Rajam, Surface and Coatings Technology, 201 (2006) 2193.
16. "Corrosion Costs and Preventive Strategies in the United States", U.S. Department of Transportation, Publication No. FHWA-RD-01-156, 2002.
17. M. Cox, "Better, lighter weapons", Army Times, 28 May 2007, pp. 14.
18. G.R. Kramlich, D.L. Henderson, S.R. Goerger, "Predicting Remaining Effective Life in Small Arm Weapons", DTIC Report No. ADB326955, May 2007.
19. D.J. Helfritch, S.M. Grendahl, and B.E. Placzankis, "Laboratory Test and Evaluation for Small-Arms Lubricants", ARL Report No. ARL-TR-3522, June 2005.